catalysts

MDPI

Article

Palladium Nanoparticles Supported on Triphenylphosphine-Functionalized Porous Polymer as an Active and Recyclable Catalyst for the Carbonylation of Chloroacetates

Yali Wan [1], Zaifei Chen [2], Dingfu Liu [1,*] and Yizhu Lei [2,*]

[1] School of Chemistry and Chemical Engineering, Guizhou University, Guiyang, Guizhou 550025, China; ylwanabc@163.com

[2] School of Chemistry and Materials Engineering, Liupanshui Normal University, Liupanshui, Guizhou 553004, China; zfei1993@163.com

* Correspondence: liudfgu@163.com (D.L.); yzleiabc@126.com (Y.L.); Tel.: +86-085-8860-0172 (Y.L.)

Received: 2 November 2018; Accepted: 22 November 2018; Published: 26 November 2018

Abstract: Dialkyl malonates are important organic intermediates that are widely used as building blocks in organic synthesis. Herein, palladium nanoparticles supported on a triphenylphosphine-functionalized porous polymer were successfully developed as an efficient and recyclable catalyst for the synthesis of dialkyl malonates via the catalytic carbonylation of chloroacetates. The influence of reaction parameters such as solvent, base, and promoter on activity was carefully investigated. With a 1 mol% of palladium usage, excellent yields of dialkyl malonates were obtained. Importantly, the catalyst can be easily separated and reused at least four times, without a significant loss in reactivity. Furthermore, the developed catalyst was also highly active for the alkoxycarbonylation of α-chloro ketones.

Keywords: carbonylation; malonate; palladium; porous organic polymer; triphenylphosphine; organic chloride

1. Introduction

Carbonylative transformation of organic halides using palladium catalysts represents a versatile method for the synthesis of carboxylic acid and its derivatives [1–4]. Carbon monoxide, an inexpensive and readily available C_1 building block, is widely used as a carbonyl source for the palladium-catalyzed carbonylation of aryl halides [5–12]. However, except as a cheap carbonyl source, CO could also act as a strong π-acidic ligand for the palladium metal, thus resulting in a decrease of electron density for the palladium center and making the oxidative addition of aryl halide difficult [13,14]. As such, the carbonylation reaction of organic halides is usually more difficult than corresponding non-carbonylative reactions, especially for those reactions where the oxidative addition of the carbon-halide bond is the rate-determining step. Meanwhile, under a CO atmosphere, the palladium atom is easily aggregated, forming the catalytically inactive species [15,16]. To increase the catalytic activity and stability of palladium catalysts in carbonylation reactions, electron-rich ligands are usually needed [17,18].

Homogeneous palladium complexes usually show high catalytic activity and selectivity [1–4,19–22]; however, they still suffer from some drawbacks, such as problems of catalyst separation and reuse [23]. Heterogeneous switching of a homogeneous palladium complex by immobilizing the complex or nanoparticle onto the solid support has been expected to address these problems [14–25], where traditional polymers and silicas are the most widely used support materials [26]. However,

these traditional supports "anchored" palladium catalysts often suffer from poor stability and inhomogeneously distributed active sites [27]. Moreover, under a CO atmosphere, palladium supported on these traditional supports is easily aggregated, forming catalytically inactive species during the reactions and thus lowering their stability and catalytic activities [16]. Therefore, developing a heterogeneous catalytic system, which has high catalytic activity and an excellent stability, is worthy of further study.

Porous organic polymers (POPs), which feature a high surface area, excellent stabilities, a designable chemical structure, and a flexible synthetic strategy, have attracted tremendous interest recently because of their potential applications in catalysis, adsorption, separation, gas storage, and other fields [28,29]. In recent years, a series of POPs containing a PPh_3 ligand and its derivatives, have been successfully prepared and applied as catalysis supports for immobilizing transition metals [30–34]. Due to the strong interaction between transition metals and phosphine ligands, these catalysts usually exhibit high catalytic activities, long-term reusability, and excellent leaching resistant ability [30–37]. Some of them have even outperformed the activities of their homogeneous analogues [30,35–37]. Although the applications of phosphine functionalized POPs in non-carbonylative cross-coupling reactions of organic halides have been widely investigated in recent years [30,34,36,37], studies of their catalytic applications in the carbonylation of organic halides are relatively unexplored [38].

Dialkyl malonates are important organic intermediates that are widely used as building blocks for the synthesis of vitamins, pharmaceuticals, agrochemicals, and so on [39]. To continue our ongoing efforts for exploring efficient catalysts for the synthesis of dialkyl malonate [40], herein, we reported palladium nanoparticles supported on a triphenylphosphine-functionalized porous polymer (PdNPs@POP-Ph_3P) as an active and recyclable catalyst for the carbonylation of chloroacetates.

2. Results and Discussion

2.1. Characterization of the Catalyst

Nitrogen adsorption-desorption analysis of POP-PPh_3 showed that the prepared POP-PPh_3 has a 1146 $m^2 \cdot g^{-1}$ BET surface area with a high pore volume (Table 1, entry 1). After immobilization of the palladium metal, the obtained PdNPs@POP-Ph_3P still preserved a high BET surface area of 987 $m^2 \cdot g^{-1}$ and a high pore volume of 1.92 cm^3/g. The sorption isotherms of the samples (Figure 1) exhibited combined type I and type IV sorption behaviour. The steep increase at a low relative pressure ($P/P_0 < 0.01$) indicates the filling of micropores, the hysteresis loop at the relative pressure of 0.7–1.0 implies the presence of mesopores, and the sharp rise at the relative pressure of 0.8–1.0 indicates the presence of macropores. Correspondingly, the pore size distribution curve (inset) of PdNPs@POP-Ph_3P also indicates its hierarchical pore structure.

Table 1. Textural properties of the prepared samples.

Entry	Catalysts	SBET ($m^2 \cdot g^{-1}$)	Pore Volume (cm^3/g) [1]	Average Pore Radius (nm) [2]
1	POP-PPh_3	1146	2.41	8.42
2	PdNPs@POP-PPh_3	987	1.92	6.50

[1] Single point adsorption total pore volume of pores at $P/P_o = 0.99$. [2] Adsorption average pore diameter (4V/A by BET).

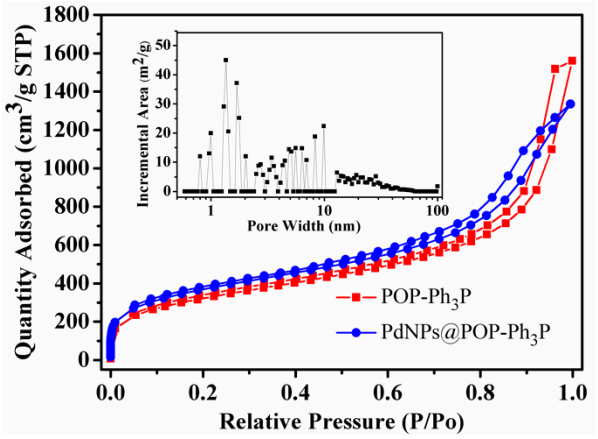

Figure 1. Nitrogen adsorption-desorption isotherms of POP-Ph_3P (square) and PdNPs@ POP-Ph_3P (circle), and pore size distribution curves (insert) of PdNPs@POP-Ph_3P.

The morphology of POP-Ph_3P and PdNPs@POP-Ph_3P was further characterized by SEM and TEM. The SEM images in Figure 2a,b suggested that POP-Ph_3P and PdNPs@POP-Ph_3P were comprised of loosely packed and irregular-shape nanoparticles. A representative TEM image (Figure 2c) of POP-Ph_3P further confirmed the presence of mesopores in the polymer. The TEM image (Figure 2d) of PdNPs@POP-Ph_3P showed the formation of well-dispersed Pd nanoparticles with a relatively narrow size distribution. As depicted in Figure 3, the average diameter of Pd clusters was about 2.9 nm.

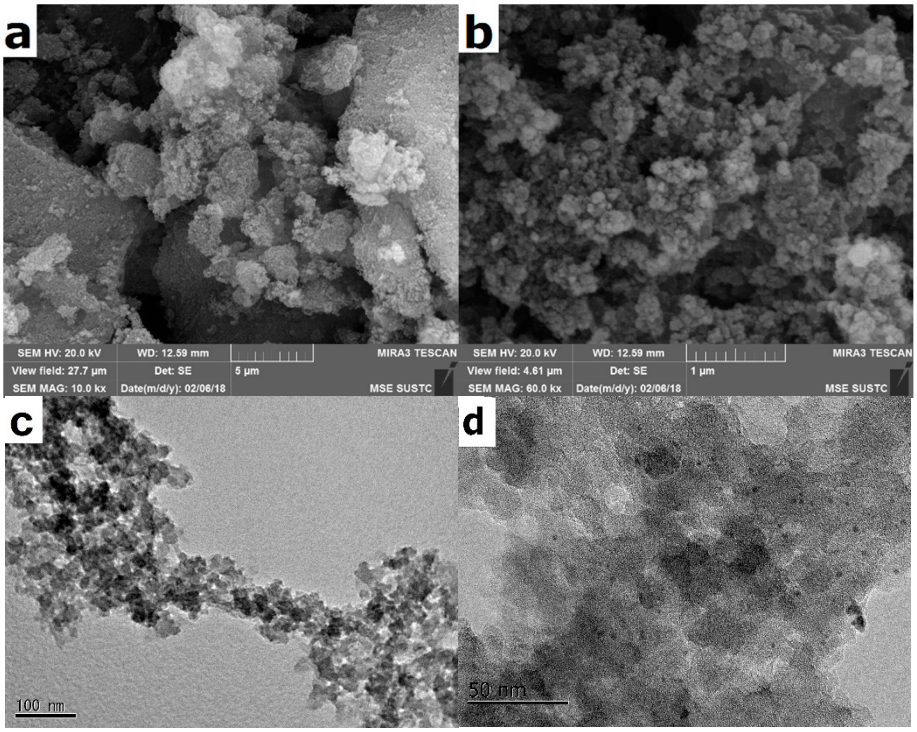

Figure 2. SEM images of POP-Ph_3P (**a**) and PdNPs@ POP-Ph_3P (**b**); TEM images of POP-Ph_3P (**c**) and PdNPs@ POP-Ph_3P (**d**).

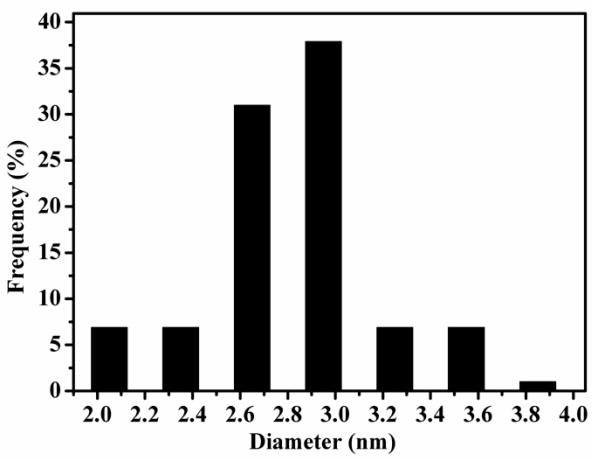

Figure 3. Particle size distribution of palladium nanoparticles on PdNPs@ POP-Ph_3P.

FT-IR spectra of 3V-PPh_3 and POP-Ph_3P are shown in Figure 4. The results revealed that the stretching band of C=C (1627 cm^{-1}) disappeared after the polymerization reaction. It indicated that the polymerization of vinyl groups had finished. The characteristic P-Ar stretching vibration (1442 cm^{-1}) also suggested the successful incorporation of the phosphine ligand in the polymer [41,42].

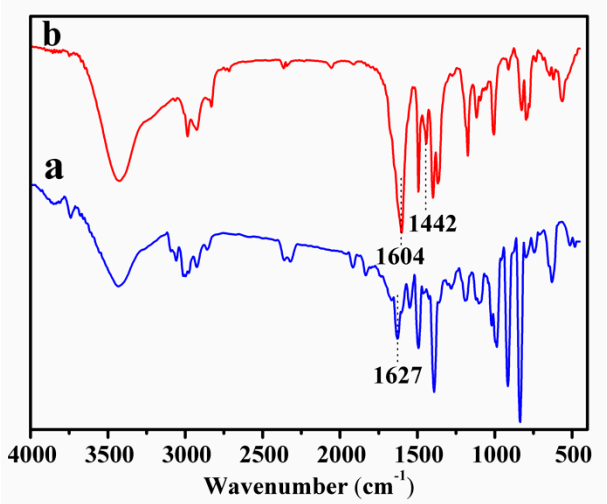

Figure 4. FTIR spectra of 3V-Ph_3P (**a**) and POP-Ph_3P (**b**).

XPS analysis was used to study the composition of POP-Ph_3P and PdNPs@POP-Ph_3P. As shown in Figure 5, P and C elements are present in the two samples. Compared with the POP-Ph_3P polymer, an additional Pd band was observed in the XPS full spectrum of PdNPs@POP-Ph_3P. The XPS spectrum of Pd 3d revealed that Pd was present in a zero state. As shown in Figure 6a, the binding energy of Pd $3d_{5/2}$ was about 334.9 eV, which was about 0.5 eV lower than that of free Pd^0 (335.4 eV) [42]. Simultaneously, the P 2p binding energy of PdNPs@POP-Ph_3P was about 0.3 eV higher than that (131.7 eV) of POP-Ph_3P (Figure 6b). These results indicated that there was a strong coordination effect between P and Pd nanoparticles [30,36,37].

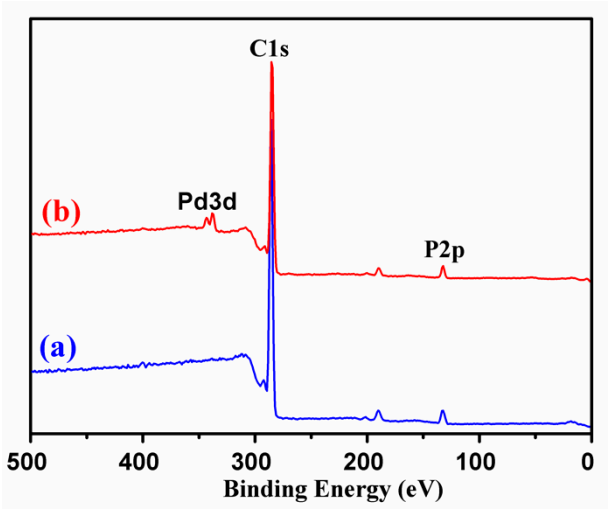

Figure 5. XPS full spectra of POP-Ph_3P (**a**) and PdNPs@ POP-Ph_3P (**b**).

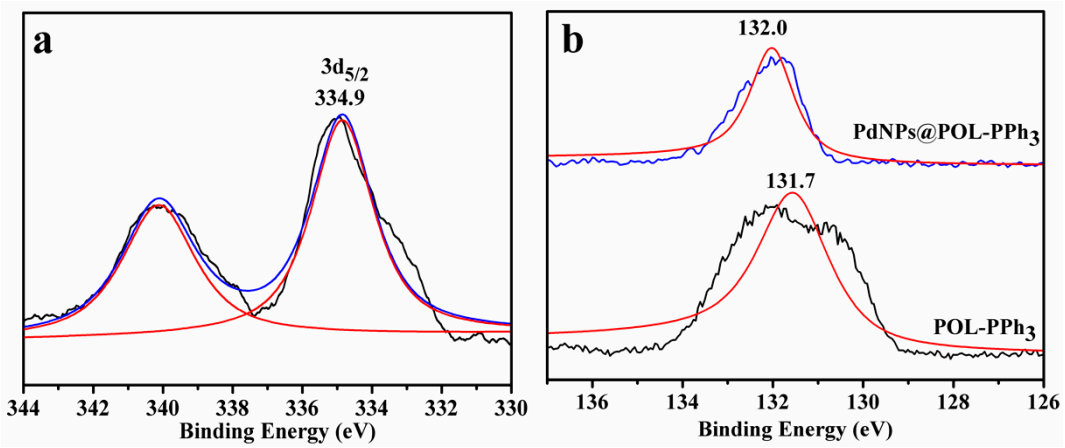

Figure 6. Pd 3d XPS spectrum of PdNPs@POP-Ph_3P (**a**), P 2p XPS spectra of POP-Ph_3P and PdNPs@ POP-Ph_3P (**b**).

2.2. Alkoxycarbonylation Reactions

With the catalyst in hand, we started our investigation with the carbonylation of ethyl chloroacetate (ECA) as a model reaction. Previous results [39,40] showed that the solvent and base have great impacts on the activity and selectivity of this carbonylation reaction. Hence, the effect of solvent and base was first investigated. As shown in Table 2, the reaction was carried out with various solvents (entries 1–9), such as ethanol, anisole, 1,4-dioxane, toluene, and 1,2-diethoxyethane (1,2-DEE). Among them, 1,2-DEE afforded the highest selectivity of diethyl malonate (97.0%), with a high conversion (83.9%) of ethyl chloroacetate (entry 6). Notably, ethanol and THF gave the higher conversions; however, the inferior selectivity of diethyl malonate (DEM) was observed (entries 1 and 9). With 1,2-DEE as the solvent, several bases were screened (entries 10–13). For base screening, Na_2HPO_4 displayed the best performance (entry 6). For comparison, the commercial Pd/C was also tested under identical reaction conditions. However, Pd/C only provided a 21.3% conversion of ethyl chloroacetate.

Previous research [39,40] suggested that the iodide promoter could extensively enhance the catalytic activity of this reaction. Therefore, the effect of a promoter was investigated (Table 3). Without any promoter, a 16.5% yield of diethyl malonate was gained (entry 1). Replacing Bu_4NI with an equal amount of Bu_4NBr or Bu_4NCl, a low or non-promotion effect was observed (entries 3 and 4). Notably, with the replacement of Bu_4NI with Et_4NI and Me_4NI, much higher conversions were achieved (entries 5 and 6). In contrast to this, the inorganic KI and NaI afforded relatively low yields,

probably due to the low solubility of the reaction solvent (entries 7 and 8). With an optimal promotion in hand, the influence of the amount of Me_4NI was further studied (entries 9–11). The results showed that a 93.8% conversion of ethyl chloroacetate could be obtained when the molar ratio of Me_4NI was increased to 15% (entry 10). However, the presence of excess Me_4NI afforded a little lower yield of diethyl malonate (entry 11). When the reaction time was further prolonged to 9 h, a high yield (94.9%) of diethyl malonate was obtained (entry 12), which was a little bit higher than that of a previously reported homogeneous and colloid catalyst [39,40]. Under the optimal conditions, we tried to lower the CO pressure, while a slight decrease in yield was observed (entry 13).

Table 2. Ethoxycarbonylation of ethyl chloroacetate: effect of solvent and base [1].

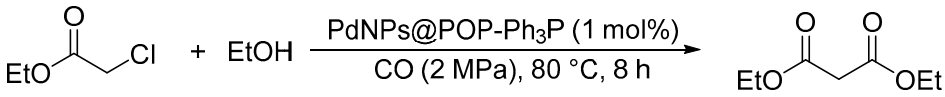

Entry	Catalyst	Solvent	Base	Conv. (mol%) [2]	Sel. (mol%)	Yield (mol%) [3]
1	PdNPs@POP-Ph_3P	ethanol	Na_2HPO_4	99.8	40.7	40.6
2	PdNPs@POP-Ph_3P	anisole	Na_2HPO_4	67.5	95.2	64.3
3	PdNPs@POP-Ph_3P	1,4-dioxane	Na_2HPO_4	82.6	85.6	70.7
4	PdNPs@POP-Ph_3P.	toluene	Na_2HPO_4	37.9	92.4	35.0
5	PdNPs@POP-Ph_3P	DGDE	Na_2HPO_4	75.1	95.7	71.9
6	PdNPs@POP-Ph_3P	1,2-DEE	Na_2HPO_4	83.9	97.0	81.4
7	PdNPs@POP-Ph_3P	1,2-DME	Na_2HPO_4	81.0	95.4	77.3
8	PdNPs@POP-Ph_3P	TEOF	Na_2HPO_4	82.4	96.5	79.5
9	PdNPs@POP-Ph_3P	THF	Na_2HPO_4	94.1	85.0	80.0
10	PdNPs@POP-Ph_3P	1,2-DEE	K_2CO_3	95.6	88.2	84.3
11	PdNPs@POP-Ph_3P	1,2-DEE	K_3PO_4	99.9	90.5	90.4
12	PdNPs@POP-Ph_3P	1,2-DEE	K_2HPO_4	64.7	94.8	61.3
13	PdNPs@POP-Ph_3P	1,2-DEE	$NaHCO_3$	51.4	79.1	40.7
14 [4]	Pd/C	1,2-DEE	Na_2HPO_4	21.3	96.1	20.5
15 [5]	$Pd(PPh_3)_2Cl_2$	1,2-DEE	Na_2HPO_4	91.6	96.7	88.6

[1] Reaction condition: PdNPs@POP-Ph_3P (125 mg, 0.02 mmol Pd), Bu_4NI (0.2 mmol), base (4 mmol), ethyl chloroacetate (2 mmol), EtOH (4 mmol), solvent (3 mL), CO (2 MPa), 80 °C, 8 h, stirring speed (800 rpm). [2] Conv. $= \frac{n_0-n_1}{n_0} \times 100\%$ (n_0 and n_1 represent the molar number of the added and remanent ECA before and after the reaction). [3] Yield $= \frac{n_{DEM}}{n_0} \times 100\%$. [4] Pd/C (42 mg, 0.02 mmol Pd). [5] $Pd(PPh_3)_2Cl_2$ (14 mg, 0.02 mmol).

Table 3. Carbonylation of ethyl chloroacetate: effect of promoters [1].

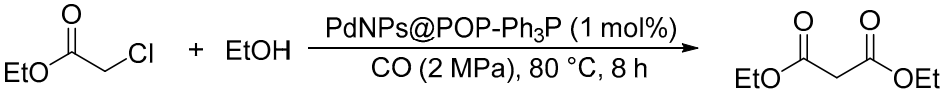

Entry	Promoter	Amount (mol%) [2]	Conv. (mol%) [3]	Sel. (mol%)	Yield (mol%) [4]
1	-	-	17.5	94.4	16.5
2	Bu_4NI	10	83.9	97.0	81.4
3	Bu_4NBr	10	29.7	95.9	28.5
4	Bu_4NCl	10	14.8	96.1	14.2
5	Et_4NI	10	87.5	97.1	85.0
6	Me_4NI	10	89.6	97.2	87.1
7	NaI	10	47.1	96.9	45.6
8	KI	10	50.3	96.9	48.7
9	Me_4NI	5	59.2	96.8	57.3
10	Me_4NI	15	93.8	97.2	91.2
11	Me_4NI	20	94.0	96.4	90.6
12 [5]	Me_4NI	15	97.7	97.1	94.9
13 [5,6]	Me_4NI	15	93.2	96.6	90.0

[1] Reaction condition: PdNPs@POP-Ph_3P (125 mg, 0.02 mmol Pd), promoter, Na_2HPO_4 (4 mmol), ethyl chloroacetate (2 mmol), EtOH (4 mmol), 1,2-DEE (3 mL), CO (2 MPa), 80 °C, 8 h, stirring speed (800 rpm). [2] Mole ratio (promoter/ethyl chloroacetate). [3] Conv. $= \frac{n_0-n_1}{n_0} \times 100\%$ (n_0 and n_1 represent the molar number of the added and remanent ECA before and after the reaction). [4] Yield $= \frac{n_{DEM}}{n_0} \times 100\%$. [5] Reaction time (9 h). [6] CO (1 MPa).

In addition to catalytic activity, the recovery and reusability of the catalyst are also crucial in the evaluation of the economic feasibility of a catalytic process. The reusability and stability of PdNPs@POP-Ph_3P were evaluated under the optimal conditions. After each run, the catalyst was recovered by centrifugation and washed with 1,2-DEE. The obtained liquid was quantitatively analysed using GC. As shown in Figure 7, the catalyst could be effectively reused at least four times, with only slight loss in its activity. Moreover, ICP analysis suggested that the palladium loading of the recycled PdNPs@POP-Ph_3P after being reused four times was 1.61 wt%, indicating that 95% of palladium on PdNPs@POP-Ph_3P was preserved during the recycling.

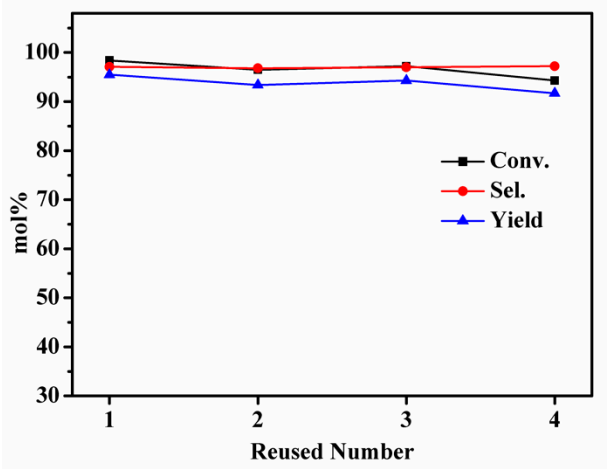

Figure 7. Reuse of PdNPs@POP-Ph_3P. Reaction condition: PdNPs@POP-Ph_3P (125 mg, 0.02 mmol Pd), Me_4NI (0.3 mmol), Na_2HPO_4 (4 mmol), ethyl chloroacetate (2 mmol), EtOH (4 mmol), 1,2-DEE (3 mL), CO (2 MPa), 80 °C, 9 h, stirring speed (800 rpm).

Then, we turned our focus to the general applicability of this catalytic system (Table 4). The carbonylation of methyl chloroacetate with methanol could proceed smoothly under the optimized conditions, and an excellent yield (95.8%) of dimethyl malonate was achieved (entry 1). Interestingly, some mixed-alkyl malonates were also prepared in excellent yields under the reaction conditions (entries 2–4), although a competing transesterification reaction with the chloroacetate substrate or with the malonate product was possible. Alkoxycarbonylation of α-chloro ketones represents a valuable alternative for the synthesis of the useful β-keto esters [43]. Considering the similar structure of α-chloro ketones and chloroacetates, the alkoxycarbonylation of α-chloro ketones was also tested under the optimal catalytic system. To our delight, both α-chloroacetone and α-chlorobenzophenone reacted readily, affording corresponding β-keto esters in high yields within 4 h (entries 5–8).

Table 4. Alkoxycarbonylation of chloroacetates and α-chloro ketones [1].

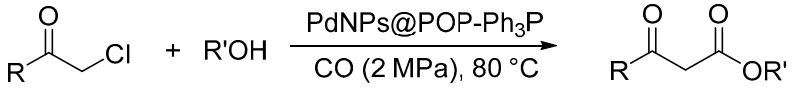

Entry	Organic Chloride	ROH	t (h)	Product	Con. (mol%) [2]	Sel. (mol%)	Yield (mol%) [3]
1	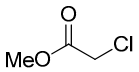	MeOH	9	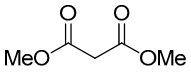	98.5	97.3	95.8
2	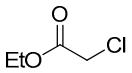	MeOH	9	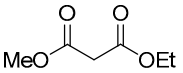	98.2	95.3	93.6
3	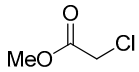	EtOH	9	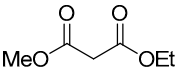	97.6	94.8	92.5

Table 4. *Cont.*

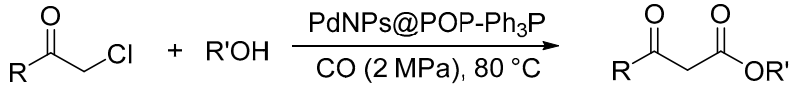

Entry	Organic Chloride	ROH	t (h)	Product	Con. (mol%) [2]	Sel. (mol%)	Yield (mol%) [3]
4	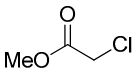	*i*-PrOH	12	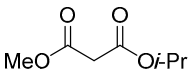	97.0	96.0	93.1
5	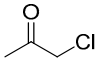	MeOH	2	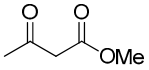	99.5	99.0	98.5
6	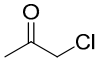	EtOH	2	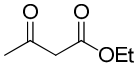	99.2	99.2	98.4
7		*i*-PrOH	2	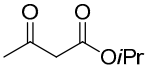	93.8	97.8	91.7
8	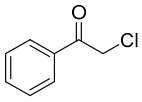	EtOH	4	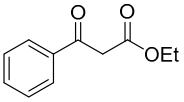	99.4	93.6	93.0

[1] Reaction condition: PdNPs@POP-Ph_3P (125 mg, 0.02 mmol Pd), Me_4NI (0.3 mmol), Na_2HPO_4 (4 mmol), chloroacetate or α-chloro ketones (2 mmol), ROH (4 mmol), 1,2-DEE (3 mL), CO (2 MPa), 80 °C, stirring speed (800 rpm). [2] Conv. $= \frac{n_0-n_1}{n_0} \times 100\%$ (n_0 and n_1 represent the molar number of the added and remanent ECA before and after the reaction). [3] Yield $= \frac{n_t}{n_0} \times 100\%$. n_0 = mole number of added chloride, n_1 = mole number of target product.

3. Materials and Methods

3.1. Materials

4-Bromostyrene, phosphorus trichloride, 2,2′-azobis(2-methylpropionitrile) (AIBN), and palladium acetate (99%) were obtained from Energy Chemical Co. Ltd. (Shanghai, China). Chloroacetates, chloroacetones, methanol, ethanol, 1,2-dimethoxyethane (1,2-DME), 1,2-diethoxyethane (1,2-DEE), diethylene glycol dimethyl ether (DGDE), triethyl orthoformate (TEOF), isopropanol, and bases were of analytical grade and used as received. CO and Ar with the purity of 99.99% were obtained from a local manufacturer. Pd/C (palladium content, 5 wt%) was supplied by Shaanxi Rock New Materials Co. Ltd. (China). Tris(4-vinylphenyl)phosphane (3V-PPh_3) was prepared according to the procedures reported in the literature [35]. Tris(4-vinylphenyl)phosphane, ^{1}H NMR (400 MHz, DMSO-d_6): δ = 7.59–7.41 (6 H, m), 7.31–7.14 (6 H, m), 6.74 (3 H, dd, *J* = 17.8, 11.0 Hz), 5.87 (3 H, dd, *J* = 17.7, 1.0 Hz), 5.31 (3 H, dd, *J* = 10.9, 1.0 Hz) ppm; ^{13}C NMR (100 MHz, DMSO-d_6) δ = 137.7, 136.2, 136.0, 133.4, 133.4, 126.5, 126.4, 115.4 ppm.

3.2. Preparation of the Porous Polymer (POP-Ph_3P)

POP-Ph_3P was obtained according to the synthetic procedures reported by the literature [31], with slight modifications. The polymerization reaction was carried out in a stainless-steel autoclave (Teflon-lined). Generally, tris(4-vinylphenyl)phosphane (3V-PPh_3, 2.0 g) and AIBN (50 mg) were dissolved in THF (20 mL) in a 100 mL Teflon lining. After replacing air in the Teflon lining with Ar for 5 min (1 L/min), the Teflon lining was transferred into an autoclave, and heated in an oven at 100 °C for 24 h. After the polymerization reaction, the obtained white solid monolith was washed with ethanol five times, and then dried under vacuum (60 °C).

3.3. Preparation of Catalysts

In a typical synthesis, POP-Ph_3P (1.0 g) was added to 30 mL methanol containing 43 mg of palladium acetate (99%). After stirring at room temperature for 12 h, 10 mL of methanol solution containing 290 mg of $NaBH_4$ was added into the above solution. The resulting mixture was vigorously stirred for 6 h. PdNPs@POP-Ph_3P was obtained after filtration and washed with methanol. ICP analysis suggested that the prepared PdNPs@POP-Ph_3P has a 1.70 wt% palladium loading.

3.4. Alkoxycarbonylation of Chloroacetates and Chloracetone

In a 50 mL Teflon-lined stainless-steel autoclave, PdNPs@POP-Ph_3P (0.02 mmol Pd), Bu_4NI (0.3 mmol), Na_2HPO_4 (4 mmol), 1,2-DEE (3 mL), organic chloride (2 mmol), and alcohol (4.0 mmol) were added into the reactor. After purging four times with CO, the autoclave was pressurized with CO to 2.0 MPa. Then, the reaction was reacted at 80 °C for a definite time. After that, the autoclave was cooled to room temperature and carefully depressurized. The catalyst was separated by centrifugation at 8000 rpm for 10 min and washed with 1,2-DEE. The liquid mixture was collected and analyzed qualitatively by GC and GC-MS as reported in the literature [39,40]. All the prepared esters are known products, which we have reported previously [40].

3.5. Characterization

Nitrogen physisorption measurements were carried out at 77 K on a Micrometrics ASAP 2020 system (Norcross, USA), and the samples were treated under vacuum at 90 °C for 10 h before the measurements. The surface area and pore size distribution were calculated by the Brunauer-Emmett-Teller (BET) and nonlocal density functional theory (NLDFT) methods, respectively. Fourier transform infrared (FTIR) spectra were recorded on a Bruker Equinox 55 FTIR spectrophotometer (Karlsruhe, Germany). The morphology of the sample was observed with a TESCAN MIRA3 field emission scanning electron microscope (FE-SEM, Brno, Czech) and a FEI Tecnai G2 F30 transmission electron microscope (TEM, Hillsboro, USA). X-ray photoelectron spectroscopy (XPS) experiments were carried out over a VG multilab 2000 spectrometer (Massachusetts, USA) fitted with a Mg-Al_{Ka} X-ray source. The amount of palladium loading and leaching was determined by inductively coupled plasma atomic emission spectroscopy (ICP, PerkinElmer Optima 8000, Massachusetts, USA). Gas chromatography (GC) was performed on a Scientific™ TRACE™ 1310 (Massachusetts, USA) equipped with a TRACE TR-WAX capillary column (Massachusetts, USA) and an FID.

4. Conclusions

In conclusion, we have developed an active and recyclable catalyst for the synthesis of malonates via the carbonylation of chloroacetates. Under the optimal condition, the solid catalyst displayed high catalytic activity, affording corresponding dialkyl malonates and mixed-alkyl malonates in high yields. Importantly, the catalyst was quite robust, and could be reused four times with only an appreciable leaching of palladium species. Furthermore, the developed catalyst also showed high catalytic activities for the alkoxycarbonylation of α-chloro ketones. Thus, this protocol not only provides an active heterogeneous catalyst for the alkoxycarbonylation of chloroacetates and α-chloro ketones, but also provides some clues to develop efficient heterogeneous catalysts for other carbonylation reactions.

Author Contributions: D.L., Y.L. and Y.W. designed the experiments; Y.W. and Z.C. performed the experiments and analyzed the data; Y.W., D.L. and Y.L. wrote the paper.

Funding: This work is financial supported by the National Natural Science Foundation of China (No. 21763017), the Youth Talent Growth Project of Educational Department of Guizhou Province (qian jiao he KY [2016]264), the Natural Science Foundation of Guizhou Province (qian ke he ji chu [2018]1414 and [2016]1133), the Liupanshui Key Laboratory of High Performance Fibers and Advanced Porous Materials (52020-2017-02-02 and 52020-2018-03-02), and the Funds of Liupanshui Normal University (LPSSYKJTD201501 and LPSSYZDXK201602).

Conflicts of Interest: The authors declare no conflict of interest.

References

1. Peng, J.B.; Qi, X.; Wu, X.-F. Recent achievements in carbonylation reactions: A personal account. *Synlett* **2017**, *28*, 175–194.
2. Friis, S.D.; Lindhardt, A.T.; Skrydstrup, T. The development and application of two-chamber reactors and carbon monoxide precursors for safe carbonylation reactions. *Acc. Chem. Res.* **2016**, *49*, 594–605. [CrossRef] [PubMed]
3. Wu, X.-F.; Neumann, H.; Beller, M. Synthesis of heterocycles via palladium-catalyzed carbonylations. *Chem. Rev.* **2012**, *113*, 1–35. [CrossRef] [PubMed]
4. Wu, X.-F.; Neumann, H.; Beller, M. Palladium-catalyzed carbonylative coupling reactions between Ar–X and carbon nucleophiles. *Chem. Soc. Rev.* **2011**, *40*, 4986–5009. [CrossRef] [PubMed]
5. Peng, J.B.; Wu, F.P.; Xu, C.; Qi, X.; Ying, J.; Wu, X.-F. Direct synthesis of benzylic amines by palladium-catalyzed carbonylative aminohomologation of aryl halides. *Commun. Chem.* **2018**, *1*, 29. [CrossRef]
6. Lagueux-Tremblay, P.L.; Fabrikant, A.; Arndtsen, B.A. Palladium-catalyzed carbonylation of aryl chlorides to electrophilic aroyl-DMAP salts. *ACS Catal.* **2018**, *8*, 5350–5354. [CrossRef]
7. Shen, C.; Fink, C.; Laurenczy, G.; Dyson, P.J.; Wu, X.-F. Versatile palladium-catalyzed double carbonylation of aryl bromides. *Chem. Commun.* **2017**, *53*, 12422–12425. [CrossRef] [PubMed]
8. Lei, Y.; Xiao, S.; Li, G.; Gu, Y.; Wu, H.; Shi, K. Mild and efficient Pd $(P^tBu_3)_2$-catalyzed aminocarbonylation of aryl halides to aryl amides with high selectivity. *Appl. Organometal. Chem.* **2017**, *31*, e3637. [CrossRef]
9. Li, Y.; Wu, X.-F. Copper/iron co-catalyzed alkoxycarbonylation of unactivated alkyl bromides. *Commun. Chem.* **2018**, *1*, 39. [CrossRef]
10. Li, Y.; Wang, Z.; Wu, X.F. A sustainable procedure toward alkyl arylacetates: Palladium-catalysed direct carbonylation of benzyl alcohols in organic carbonates. *Green Chem.* **2018**, *20*, 969–972. [CrossRef]
11. Li, Y.; Wang, Z.; Wu, X.F. Palladium-catalyzed carbonylative direct transformation of benzyl amines under additive-free conditions. *ACS Catal.* **2017**, *8*, 738–741. [CrossRef]
12. Li, Y.; Zhu, F.; Wang, Z.; Rabeah, J.; Brückner, A.; Wu, X.F. Practical and general manganese-catalyzed carbonylative coupling of alkyl iodides with amides. *ChemCatChem* **2017**, *9*, 915–919. [CrossRef]
13. Fagnou, K.; Lautens, M. Halide effects in transition metal catalysis. *Angew. Chem. Int. Ed.* **2002**, *41*, 26–47. [CrossRef]
14. Sargent, B.T.; Alexanian, E.J. Palladium-catalyzed alkoxycarbonylation of unactivated secondary alkyl bromides at low pressure. *J. Am. Chem. Soc.* **2016**, *138*, 7520–7523. [CrossRef] [PubMed]
15. Gautam, P.; Dhiman, M.; Polshettiwar, V.; Bhanage, B.M. KCC-1 supported palladium nanoparticles as an efficient and sustainable nanocatalyst for carbonylative Suzuki–Miyaura cross-coupling. *Green Chem.* **2016**, *18*, 5890–5899. [CrossRef]
16. Mei, H.; Hu, J.; Xiao, S.; Lei, Y.; Li, G. Palladium-1, 10-phenanthroline complex encaged in Y zeolite: An efficient and highly recyclable heterogeneous catalyst for aminocarbonylation. *Appl. Catal. A Gen.* **2014**, *475*, 40–47. [CrossRef]
17. Martinelli, J.R.; Clark, T.P.; Watson, D.A.; Munday, R.H.; Buchwald, S.L. Palladium-catalyzed aminocarbonylation of aryl chlorides at atmospheric pressure: The dual role of sodium phenoxide. *Angew. Chem.* **2007**, *119*, 8612–8615. [CrossRef]
18. Veige, A.S. Carbon monoxide as a reagent: A report on the role of N-heterocyclic carbene (NHC) ligands in metal-catalyzed carbonylation reactions. *Polyhedron* **2008**, *27*, 3177–3189. [CrossRef]
19. Johansson Seechurn, C.C.; Kitching, M.O.; Colacot, T.J.; Snieckus, V. Palladium-catalyzed cross-coupling: A historical contextual perspective to the 2010 Nobel Prize. *Angew. Chem. Int. Ed.* **2012**, *51*, 5062–5085. [CrossRef] [PubMed]
20. Li, Y.; Hu, Y.; Wu, X.-F. Non-noble metal-catalysed carbonylative transformations. *Chem. Soc. Rev.* **2018**, *47*, 172–194. [CrossRef] [PubMed]
21. Zhu, C.; Yang, B.; Qiu, Y.; Bäckvall, J.E. Highly selective construction of seven-membered carbocycles by olefin-assisted palladium-catalyzed oxidative carbocyclization-alkoxycarbonylation of bisallenes. *Angew. Chem. Int. Ed.* **2016**, *55*, 14405–14408. [CrossRef] [PubMed]

22. Zhu, C.; Yang, B.; Backvall, J.E. Highly selective cascade C–C bond formation via palladium-catalyzed oxidative carbonylation-Carbocyclization-Carbonylation-Alkynylation of enallenes. *J. Am. Chem. Soc.* **2015**, *137*, 11868–11871. [CrossRef] [PubMed]
23. Mohammadi, E.; Hajilou, Z.; Movassagh, B. Multiwalled carbon nanotubes supported Pd (II)-salen complex: An effective, phosphorous-free, and reusable heterogeneous precatalyst for the synthesis of diaryl ketones. *Helv. Chim. Acta* **2016**, *99*, 747–752. [CrossRef]
24. Wang, D.; Astruc, D. Fast-growing field of magnetically recyclable nanocatalysts. *Chem. Rev.* **2014**, *114*, 6949–6985. [CrossRef] [PubMed]
25. Molnar, A. Efficient, selective, and recyclable palladium catalysts in carbon-carbon coupling reactions. *Chem. Rev.* **2011**, *111*, 2251–2320. [CrossRef] [PubMed]
26. Sun, Q.; Dai, Z.; Meng, X.; Xiao, F.-S. Porous polymer catalysts with hierarchical structures. *Chem. Soc. Rev.* **2015**, *44*, 6018–6034. [CrossRef] [PubMed]
27. Wang, C.A.; Zhang, Z.K.; Yue, T.; Sun, Y.L.; Wang, L.; Wang, W.D.; Zhang, Y.; Liu, C.; Wang, W. "Bottom-up" embedding of the jørgensen-hayashi catalyst into a chiral porous polymer for highly efficient heterogeneous asymmetric organocatalysis. *Chem. Eur. J.* **2012**, *18*, 6718–6723. [CrossRef] [PubMed]
28. Dong, K.; Sun, Q.; Meng, X.; Xiao, F.-S. Strategies for the design of porous polymers as efficient heterogeneous catalysts: From co-polymerization to self-polymerization. *Catal. Sci. Technol.* **2017**, *7*, 1028–1039. [CrossRef]
29. Tan, L.; Tan, B. Hypercrosslinked porous polymer materials: Design, synthesis, and applications. *Chem. Soc. Rev.* **2017**, *46*, 3322–3356. [CrossRef] [PubMed]
30. Li, B.; Guan, Z.; Wang, W.; Yang, X.; Hu, J.; Tan, B.; Li, T. Highly dispersed Pd catalyst locked in knitting aryl network polymers for Suzuki-Miyaura coupling reactions of aryl chlorides in aqueous media. *Adv. Mater.* **2012**, *24*, 3390–3395. [CrossRef] [PubMed]
31. Sun, Q.; Jiang, M.; Shen, Z.; Jin, Y.; Pan, S.; Wang, L.; Meng, X.; Chen, W.; Ding, Y.; Li, J.; et al. Porous organic ligands (POLs) for synthesizing highly efficient heterogeneous catalysts. *Chem. Commun.* **2014**, *50*, 11844–11847. [CrossRef] [PubMed]
32. Xu, Y.; Wang, T.; He, Z.; Zhou, M.; Yu, W.; Shi, B.; Huang, K. Honeycomb-like bicontinuous P-doped porous polymers from hyper-cross-linking of diblock copolymers for heterogeneous catalysis. *Macromolecules* **2017**, *50*, 9626–9635. [CrossRef]
33. Ding, Z.C.; Li, C.Y.; Chen, J.J.; Zeng, J.H.; Tang, H.T.; Ding, Y.J.; Zhan, Z.P. Palladium/phosphorus-doped porous organic polymer as recyclable chemoselective and efficient hydrogenation catalyst under ambient conditions. *Adv. Synth. Catal.* **2017**, *359*, 2280–2287. [CrossRef]
34. Iwai, T.; Harada, T.; Shimada, H.; Asano, K.; Sawamura, M. A polystyrene-cross-linking bisphosphine: Controlled metal monochelation and ligand-enabled first-row transition metal catalysis. *ACS Catal.* **2017**, *7*, 1681–1692. [CrossRef]
35. Sun, Q.; Dai, Z.; Liu, X.; Sheng, N.; Deng, F.; Meng, X.; Xiao, F.-S. Highly efficient heterogeneous hydroformylation over Rh-metalated porous organic polymers: Synergistic effect of high ligand concentration and flexible framework. *J. Am. Chem. Soc.* **2015**, *137*, 5204–5209. [CrossRef] [PubMed]
36. Zhou, Y.B.; Li, C.Y.; Lin, M.; Ding, Y.J.; Zhan, Z.P. A polymer-bound monodentate-P-ligated palladium complex as a recyclable catalyst for the Suzuki-Miyaura coupling reaction of aryl chlorides. *Adv. Synth. Catal.* **2015**, *357*, 2503–2508. [CrossRef]
37. Wang, X.; Min, S.; Das, S.K.; Fan, W.; Huang, K.W.; Lai, Z. Spatially isolated palladium in porous organic polymers by direct knitting for versatile organic transformations. *J. Catal.* **2017**, *355*, 101–109. [CrossRef]
38. Lei, Y.; Wu, L.; Zhang, X.; Mei, H.; Gu, Y.; Li, G. Palladium supported on triphenylphosphine functionalized porous organic polymer: A highly active and recyclable catalyst for alkoxycarbonylation of aryl iodides. *J. Mol. Catal. A Chem.* **2015**, *398*, 164–169. [CrossRef]
39. Hu, J.; Zhang, Q.; Guan, Z.; Gu, Y.; Mo, W.; Li, T.; Li, G. Palladium-catalyzed carbonylation of chloroacetates to afford malonates: Controlling the selectivity of the product in a buffer. *ChemCatChem* **2012**, *4*, 1776–1782. [CrossRef]
40. Lei, Y.; Zhang, R.; Wu, L.; Ou, Q.; Mei, H.; Li, G. $PdCl_2/Bu_4NI$: An efficient and ligand-free catalyst for the alkoxycarbonylation of organic chlorides. *J. Mol. Catal. A Chem.* **2014**, *392*, 105–111. [CrossRef]
41. Cai, R.; Ye, X.; Sun, Q.; He, Q.; He, Y.; Ma, S.; Shi, X. Anchoring triazole-gold (I) complex into porous organic polymer to boost the stability and reactivity of gold (I) catalyst. *ACS Catal.* **2017**, *7*, 1087–1092. [CrossRef]

42. Guo, M.; Li, H.; Ren, Y.; Ren, X.; Yang, Q.; Li, C. Improving catalytic hydrogenation performance of Pd nanoparticles by electronic modulation using phosphine ligands. *ACS Catal.* **2018**, *8*, 6476–6485. [CrossRef]
43. Wahl, B.; Bonin, H.; Mortreux, A.; Giboulot, S.; Liron, F.; Poli, G.; Sauthier, M. A general and efficient method for the alkoxycarbonylation of α-chloro ketones. *Adv. Synth. Catal.* **2012**, *354*, 3105–3114. [CrossRef]